Sociedade Portuguesa de Materiais

Available online at www.sciencedirect.com

ScienceDirect

Science and Technology of MATERIALS

http://ees.elsevier.com/stmat

Science and Technology of Materials 30 (2018) 60–68

Development of antimicrobial leather modified with Ag–TiO_2 nanoparticles for footwear industry

I. Carvalho [a,d,*], S. Ferdov [b], C. Mansilla [b], S.M. Marques [b], M.A. Cerqueira [c], L.M. Pastrana [c], M. Henriques [d], C. Gaidau [e], P. Ferreira [c], S. Carvalho [a,b]

[a] *SEG-CEMMPRE – Centre for Mechanical Engineering, Materials and Processes Department, University of Coimbra, 3030-788 Coimbra, Portugal*
[b] *CFUM-UP, Physics Department, University of Minho, 4800-058 Guimarães, Portugal*
[c] *INL-International Iberian Nanotechnology Laboratory, Av. Mestre José Veiga s/n, 4715-330 Braga, Portugal*
[d] *CEB, Centre of Biological Engineering, LIBRO-Laboratório de Investigação em Biofilmes Rosário Oliveira, University of Minho, Campus of Gualtar, 4710-057 Braga, Portugal*
[e] *Leather Research Department, INCDTP-Leather and Footwear Research Institute Division, Ion Minulescu St., Bucharest 031215, Romania*

Received 30 July 2017; accepted 25 September 2018

Abstract

The proposed work aims to functionalize leathers for footwear industry with antimicrobial properties based on Ag–TiO_2 nanoparticles. The synthesis of nanoparticles was carried out by the hydrothermal method with significant advantages in terms of time, energy savings and low cost. Anatase TiO_2 nanoparticles with dimensions below 10 nm were obtained as observed by X-ray diffraction and transmission electron microscopy. Fourier transform infrared spectroscopy showed that the based structure of leather was not modified by the addition of the nanoparticles. The antimicrobial activity was evaluated and it was observed that Ag containing leathers gained antimicrobial activity. In addition, the nanoparticles were found to be non-cytotoxic. This achievement, by itself, should be quite appealing to the footwear industry as it could consist in a solid value-preposition given the commonness of fungal infections promoted by humidity, poor breathability and temperature that promote the expansion of the microflora of the skin.

Keywords: Leather; Ag–TiO_2 nanoparticles; Antimicrobial activity; Cytotoxicity

1. Introduction

Fungal growth is a common problem in the leather industry, which has been typically controlled through the use of antimicrobial chemicals. However, many of these chemicals, mostly volatile organic compounds (VOCs), have been recently banned worldwide due to their carcinogenic effect and environmental toxicity. As a consequence, phenolic and heterocyclic compounds that are often used in the tanning industry as fungicides are susceptible to become unacceptable. Therefore, the development of new compounds with prolonged antifungal effect and no toxicity is of great importance [1].

Silver nanoparticles (Ag–NPs) have gained significant popularity due to their broad spectrum of antimicrobial activity [2–4], and thus have been used for therapeutic applications, such as catheters [5] and wound dressings [6], although they may readily enter into the cells. However, very few reports on the toxicity of Ag–NPs are available, which show different degrees of in vitro cytotoxicity [7,8]. Several studies have reported the application of Ag–NPs in leathers, as colloidal solutions and emulsions of Ag–NPs [9,10], via Ag–NPs microencapsulation [11], and Ag–NPs synthesis using natural polymers such pine resin or gum [12].

Titanium dioxide nanoparticles (TiO_2-NPs) are already used in various practical applications, such as water and air

* Corresponding author. Present address: SEG-CEMMPRE Mechanical Engineering Department, University of Coimbra, 3030-788 Coimbra, Portugal.
E-mail address: isascarvalho@hotmail.com (I. Carvalho).

https://doi.org/10.1016/j.stmat.2018.09.002

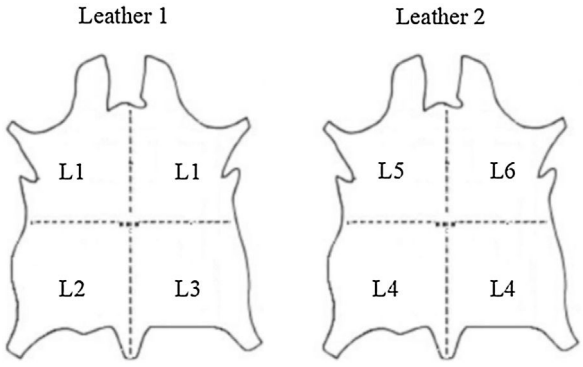

Fig. 1. Schematic showing the 4 pieces cut in each leather that were subjected to different surface base treatments summarized in Table 1. The labels L1–L6 shown in this figure will be used as identification of the substrates.

purification, self-cleaning and self-sterilizing surfaces [13–16], and optical and dielectric devices [17]. Therefore, the combination of Ag–NPs and TiO_2-NPs is intended to extend the applicability of both as a single system with enhanced properties. TiO_2 nanoparticles have been prepared by different approaches, e.g. sol gel, hydrothermal and solvothermal methods [18–22]. Therefore, in this work, a variation of the hydrothermal method for low temperatures has been developed for the synthesis of Ag–TiO_2 NPs. The main objective of this work is to evaluate the antimicrobial activity of leathers covered with Ag–TiO_2 NPs. For a realistic evaluation, different types of microorganisms were selected including a fungus strain, *Candida albicans* and two bacteria, *Pseudomonas aeruginosa* and *Staphylococcus aureus.*

2. Materials and methods

2.1. Description and preparation of leather substrates

Two leathers (labeled 1 and 2) of goat skin origin processed as shoe lining leathers were supplied by the R&D National Institute for Textile and Leather (INCDTP) – Leather and Footwear Research Institute (ICPI) Division, Romania. Both leathers were cut in 4 × 1/4 pieces, as shown in Fig. 1. The different pieces were subjected to five different surface treatments, in such a way that two pieces of each leather suffered the same treatment (pieces L1 of Leather 1 and pieces L4 of Leather 2). Pieces L2 and L5, and L3 and L6, were subjected to the same treatment, with the sole difference that in case of L5 and L6 a rutile white pigment was also included. Table 1 summarizes the description of the surface treatments performed for each piece.

Leathers 1–6 were cut in circular pieces (10 mm diameter × 1.0 mm thick). Afterwards, a cleaning treatment was performed in order to remove all the impurities, which is based on the immersion of the samples in ethanol (70%, AGA, Portugal), followed by water for a few minutes. The samples were then left to dry at room temperature and stored in a desiccator before being functionalized with TiO_2 and Ag–TiO_2 nanoparticles.

2.2. Synthesis of TiO_2 and Ag–TiO_2 NPs

The synthesis of TiO_2 nanoparticles was performed by a hydrothermal method, with significant advantages in terms of time, energy savings and low cost. A 10% (v/v) solution of titanium butoxide (97%, Aldrich) was prepared by addition to distilled water without any stirring. The solution was placed in a container that can withstand temperatures up to 70 °C (e.g. can be an autoclave or a polymeric bottle). This container was placed in an oven for 4 h at 70 °C. A white powder was obtained after filtration and drying of the solution. The Ag–TiO_2 nanoparticles, were obtained by precipitation of Ag_2O on the surface of anatase by the following reaction: $2AgNO_3 + 2NaOH \rightarrow Ag_2O + NaNO_3 + H_2O$. Therefore, 0.8 g of TiO_2 dried nanoparticles were dispersed in a solution of 0.018 g of $AgNO_3$ and 40 g of H_2O. Subsequently, a second solution of 0.08 g of NaOH and 10 g H_2O was added to the above mixture. The reaction was carried out under constant stirring at room temperature. The obtained powder of Ag–TiO_2 was filtered, washed and dried at 50 °C.

2.3. Coverage of leathers with TiO_2 and Ag–TiO_2 nanoparticles

The different pieces of leathers were covered with TiO_2 and Ag–TiO_2 NPs. Two aqueous dispersions of 4% (w/w) of each

Table 1
Description of the different surface base treatments of six sides – six samples.

Leather 1	Leather 2
Pieces L1 Leather without surface base coat. These samples are in the crust stage of processing, tanned with glutaraldehyde and syntans and re-tanned with phenol based materials.	Pieces L4
Piece L2 Leather with surface base coat finishing layer. This sample is processed in the crust stage and covered by spraying with a base coat layer of film forming acrylic polymers. In case of L5, a white rutile pigment is included in the base coat.	Piece L5
Piece L3 Leather sample treated as sample L2 and L5 with an additional application of a fixing top coat based on nitrocellulose.	Piece L6

nanoparticle were prepared, and the samples were immersed in 100 mL of each solution during 24 h at room temperature. Subsequently, the leathers were placed in the oven to dry (50 °C). Following this procedure, they were washed under water to simulate the environmental conditions of operation and to prove that the nanoparticles were successfully incorporated on the leather surface. Finally, the samples were dried at room temperature.

2.4. Nanoparticles characterization

2.4.1. Structural composition and morphological analysis

The structure of the TiO_2 and Ag–TiO_2 nanoparticles were analyzed by X-ray diffraction (XRD) using a Bruker D8 Discover diffractometer operating with Cu Kα radiation (λ = 1.5406 Å), step 0.04°, time per step 1 s and 20–60° 2θ interval. The particle size, morphology and crystallite size was characterized by transmission electron microscopy using a JEOL JEM 2100 FEG operated at an accelerating voltage of 200 kV. The samples were prepared by adding ethanol to the nanoparticles, followed by ultrasonic dispersion. Then 3–4 drops of the suspension were dried on the carbon coated copper grids for TEM analyses.

2.4.2. Cytotoxicity assay

Cytotoxicity tests for TiO_2 and Ag–TiO_2 nanoparticles were performed using 3T3 fibroblast line (CCL-163, ATCC) by an indirect contact method (nanoparticles were exposed to Dulbecco modified eagle medium, DMEM (Gibco) containing 10% of FBS (Gibco) and 1% penicillin streptomycin, P/S (Gibco) (complete DMEM) and it was extracted a little of this solution and added to cells). 10 mg of TiO_2 and Ag–TiO_2 nanoparticles (previously sterilized at UV light during 1 h) were inserted in 24 wells plates, each well containing 1 mL of complete DMEM. Then the plates were incubated with 5% CO_2 at 37 °C for 24 h. Indeed, the cells were grown in complete DMEM and allowed to grow until attaining 80% confluence and after detachment, 50 μL of cell suspension with 1×10^5 cells/mL were added to each well of a 96 wells' plate. After, the plates were also incubated with 5% CO_2 at 37 °C for 24 h. Subsequently, 50 μL of complete DMEM were extracted from each well of the 24 well plate where the nanoparticles had been inserted and added to 96 wells' plate with adhered cells. At this point, the plate was again incubated with 5% CO_2 at 37 °C for further 24 h. Then, 20 μL of MTS were pipetted to each well of the 96 wells assay plates containing the samples in 100 μl of culture medium. After 1 h, the absorbance of the resulting solution was read at 490 nm. In all performed assay, each wells' plate was examined under a phase contrast microscope to ensure that cell growth was relatively even across the plate and before addition of MTS solution to verify whether there was alteration in the cells. The percentage of cellular viability was calculated using the following expression:

$$\text{Viab.}\,(\%) = \frac{OD_{490S}}{OD_{490C}} \times 100, \quad (1)$$

where OD_{490S} means the measured value optical density of sample (cells' growth in the presence of sample) and OD_{490C} means the measured value optical density of control (cells' growth in the absence of sample). All experiments were carried out in triplicate per sample and repeated at least in three independent assays.

2.5. Leather characterization

2.5.1. Chemical and morphological analyses

Fourier Transform Infrared (FTIR) was carried out to assess whether the composition of leather remain unchanged after covering with TiO_2 and Ag–TiO_2 nanoparticles. A Bruker VERTEX 80/80 v (Boston, EUA) FTIR spectrometer was used. The analyses were performed in attenuated total reflectance (ATR) mode with a platinum crystal accessory between 900 and 4000 cm^{-1}, 16 scans, and resolution of 4 cm^{-1}.

Chemical composition was obtained with an EDAX – Pegasus X4M – energy dispersive spectrometer (EDS/EBSD) apparatus coupled with a scanning electron microscopy (SEM). The surface morphology was examined by a NanoSEM – FEI Nova 200 (FEG/SEM) equipped with a field emission gun (FEG), and operated in low vacuum mode. The micrographs were obtained with secondary (SE) and backscattered (BSE) electron detectors in low voltage differential (LVD) mode at acceleration voltages ranging between 5 and 15 kV and a working distance of around 5 mm.

2.5.2. Antimicrobial properties

The antimicrobial activity of leathers uncovered and covered with both types of nanoparticles was tested against two bacteria strains and a fungus. The bacteria used were a Gram negative and a Gram positive, *P. aeruginosa* (PAO1) ATCC 15692 and *S. aureus*, ATCC 6538 obtained from American Type Cell Collection, respectively. The fungi strain used was *C. albicans* SC5314. Zone of inhibition (ZoI) tests, adapted from Kirby–Bauer test [23], were carried out to determine the antimicrobial activity of samples. The halo size was used as a qualitative measure of the sample activity.

Initially, the inoculation of a single colony was carried out in 20 mL Tryptic soy broth (TSB, Merck) or Sabouraud Dextrose Broth (SDB, Merck) culture media for bacteria and fungi strains, respectively, and incubated at 37 °C for 18 h at 120 rpm. The cells suspension obtained was adjusted to an optical density (OD) of 1.0 at 640 nm for *P. aeruginosa* and *S. aureus* and to counting by Neubauer chamber for fungus (*C. albicans*) and properly diluted in culture media to 1×10^7 CFU mL^{-1}. The incubation of the bacteria and fungus in agar was performed using 1 mL of cell suspension added to 14 mL of cooled solution (<50 °C) Tryptic Soy Agar (TSA, Merck) or Sabouraud Dextrose Agar (SDA, Merck) respectively and placed into sterile plastic petri dishes. After medium solidification, the samples (previously sterilized by exposure of ±1 h to UV light) were placed separately on the top of an agar plate, with the treatment base side in contact with the agar, and incubated for 24 h at 37 °C. After the incubation period, the halo (zone of transparent medium, which means that there is no bacteria growth) formed around the sample was measured and photographed to record the results (images captured

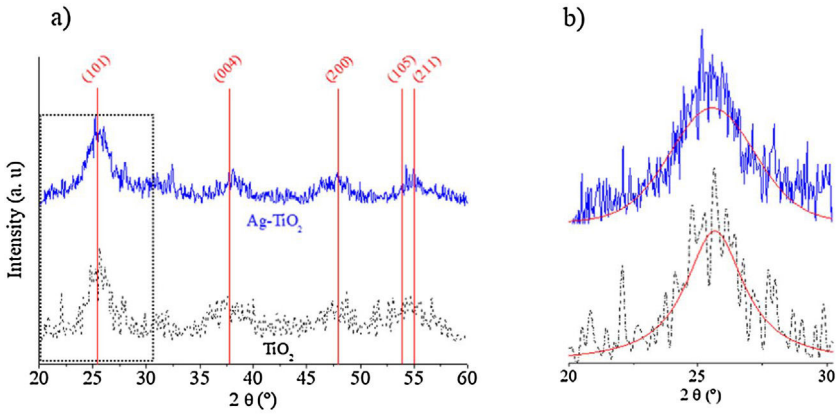

Fig. 2. (a) XRD patterns of the TiO_2 and Ag–TiO_2 powder nanoparticles. The vertical lines indicate the position of TiO_2 anatase. (b) Detailed view of the 101 peak, including the fitting employed to estimate the crystal size with the Scherrer's formula.

with Image Lab™ software). All experiments were repeated at least in three independent assays.

3. Results and discussion

3.1. Nanoparticle characterization

3.1.1. Structural composition

Fig. 2 shows the XRD diffraction patterns of TiO_2 and Ag–TiO_2 nanoparticles. The vertical lines represent the position of the tetragonal TiO_2 (ICDD 00-021-1272) anatase, which match well the formation of TiO_2 anatase. However, the peaks show a broad shape, indicating a small size of the coherent diffraction domain. In fact, a crystallite size of 4 ± 1.1 nm was determined by the Scherrer formula using the (101) peak, after a non-linear Voigt curve fit of the diffraction peaks using OriginPro 8 software.

3.1.2. Morphological analyses

Fig. 3 shows the TEM characterization of the TiO_2 nanoparticles. A low magnification image is shown in Fig. 3a. Clearly, the nanoparticles have a bi-modal size and shape distribution. The majority of the small spherical nanoparticles is around 4–10 nm, while a few larger rod-like nanoparticles in the size range of 20–60 nm can be distinguished. Fig. 3b and c show the FFT of high resolution images depicted in Fig. 3d and e, respectively, where nanoparticles of 10–15 nm can be barely distinguished. The size of the diffraction rings detected in the FFT correspond to the interplanar spaces of anatase [24]. A good agreement can be observed with the green circles in Fig. 3b and c, which indicate the theoretical position of the 101 ($d = 3.5141$ Å), 103 ($d = 2.4284$ Å), 200 ($d = 1.8911$ Å) and 105 (d = 1.6981 Å) planes of anatase [24]. The inverse FFT's of the detected diffraction points observed in Fig. 3b and c are depicted in Fig. 3f and g. In these images, the TiO_2 nanoparticles are highlighted from what was observed in Fig. 3d and e.

3.1.3. Cytotoxicity evaluation

The cytotoxicity of the nanoparticles was evaluated because these nanoparticles may easily penetrate inside the human body. This test was carried out through an MTS assay with fibroblastos 3T3, which gives an indication of the materials' viability on cells in a precise, fast and reliable way. Fig. 4 shows the cell viability in contact with TiO_2 and Ag–TiO_2 nanoparticles. All results demonstrated a viability above 70% which confirmed the non-cytotoxicity of nanoparticles, also observed in microscopy images (Fig. 4, bottom) [25].

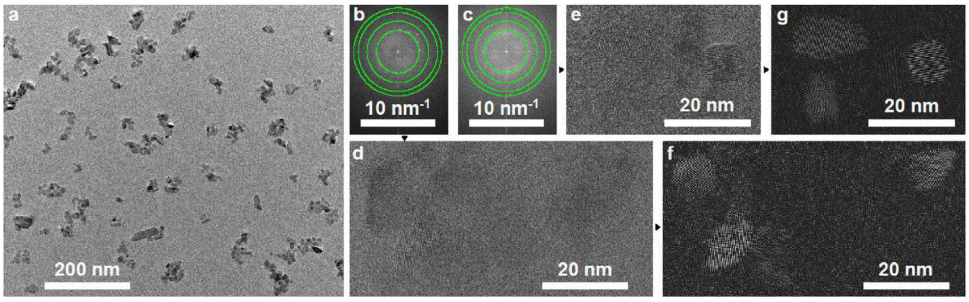

Fig. 3. TEM characterization of the TiO_2 nanoparticles. A low magnification bright-field image is shown in (a). Figures (b) and (c) represent the FFT of the high resolution images depicted in (d) and (e), respectively. The green circles associated with the diffraction rings indicate the position of the (101), (103), (200) and (105) [24] planes. The inverse FFT's of the detected diffraction rings observed in (b) and (c) are included in (f) and (g).

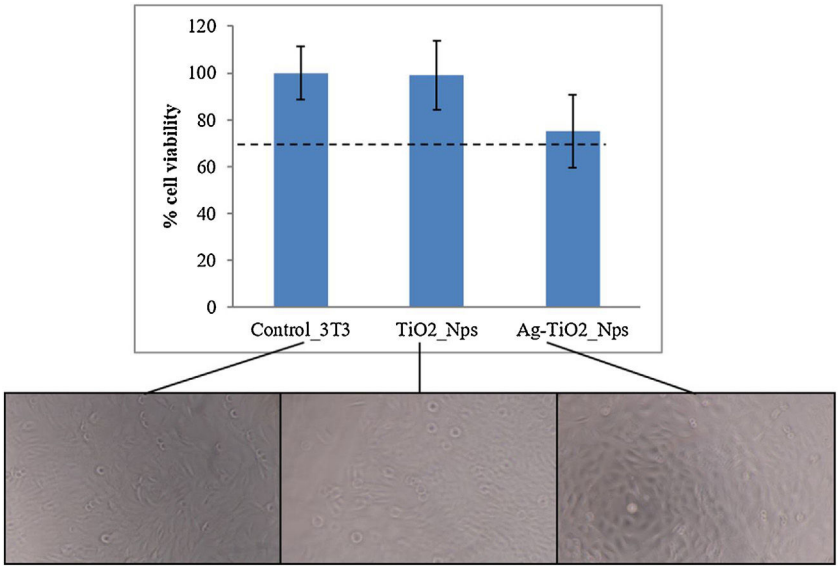

Fig. 4. Viability of 3T3 fibroblast in contact with TiO_2 and Ag–TiO_2 nanoparticles. Microscopy images of fibroblasts 3T3 examined using an inverted microscope after contact with nanoparticles.

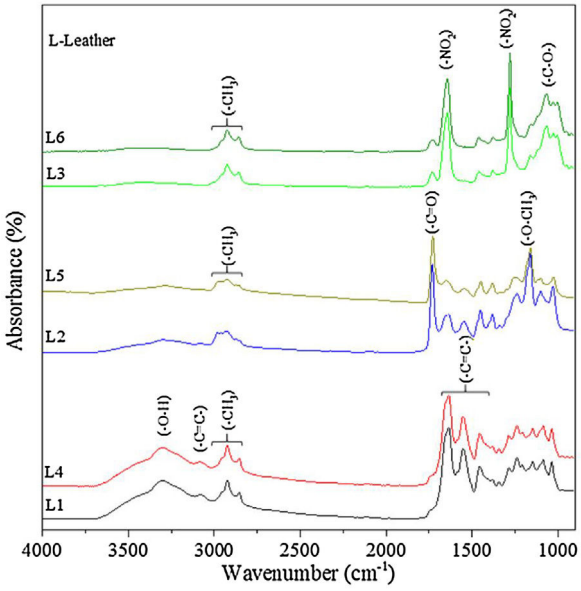

Fig. 5. FTIR spectra of six uncovered pieces of leathers (L1, L2, L3, L4, L5 and L6). Main band assignments are shown above appropriate wavenumbers.

3.2. Leather characterization before and after functionalization

3.2.1. Chemical and morphological analyses

Fig. 5 shows the FTIR spectra of six leathers before coverage with TiO_2 and Ag–TiO_2 nanoparticles. Pieces L1 and L4, L2 and L5, and L3 and L6 are very similar, in agreement with the treatment carried out (see Table 1). The unfinished pieces L1 and L4 present characteristic bands of tanning materials; at ca. 3300 cm^{-1}, a strong band is assigned to the –O–H stretching vibration of phenol; at ca. 3100 cm^{-1}, the band is attributed to =C–H stretching aromatic vibration; between ca. 3000 and 2850 cm^{-1}, the bands correspond to $–CH_3$ stretching vibration, which are visible in all leathers and ascribed to organic compounds. The three bands located at ca. 1630, 1540 and 1450 cm^{-1} are attributed to –C=C– stretching aromatic vibration [26]. Pieces L2 and L5 show typical bands attributed to esters derived of the film forming polymer applied as finishing cover. Thus, bands located at ca. 1720 cm^{-1} and 1155 cm^{-1} correspond to –C=O and $–O–CH_3$ stretching ester vibration, respectively [27]. Finally, pieces L3 and L6 show characteristic bands of the nitrocellulose used as top layer. The two intense bands observed at ca. 1640 cm^{-1} and 1280 cm^{-1} are attributed to the different vibrations of the nitrate group, namely to antisymmetric NO_2 stretching and symmetric NO_2 stretching, respectively. In the region between ca. 1100–950 cm^{-1} there are few peaks with medium intensity, which correspond to different vibrations of the CO group [28].

Fig. 6 shows FTIR spectra of the six pieces of leather prior and after covering with TiO_2 and Ag–TiO_2 nanoparticles. The results show that the nanoparticles do not modify the composition of the leather substrate. However, a certain attenuation of the bands can be observed in Fig. 6a, b, d and e when covered with nanoparticles of TiO_2 or Ag–TiO_2.

Fig. 7 shows the EDX spectra of uncovered pieces 1 to 6 (Fig. 7a) and the influence of NPs coverage on the EDX spectra of L4 (Fig. 7b).

Fig. 7a shows, intense peaks of carbon and oxygen in all leathers, which are attributed essentially to their organic composition. The sodium, silicon and sulphur peaks are ascribed to the chemical products used in the leather processing (see Table 1). Peaks of titanium can be observed in L5 and L6 as a consequence of the rutile pigment that was applied in the base finishing coat (see Table 1). These peaks are less intense in L6 probably due to the nitrocellulose fixing coating.

Fig. 7b shows the EDX spectra of L4 prior and after coverage with TiO_2 and Ag–TiO_2 NPs. As expected, both samples covered with nanoparticles show the titanium peaks. In addition, the

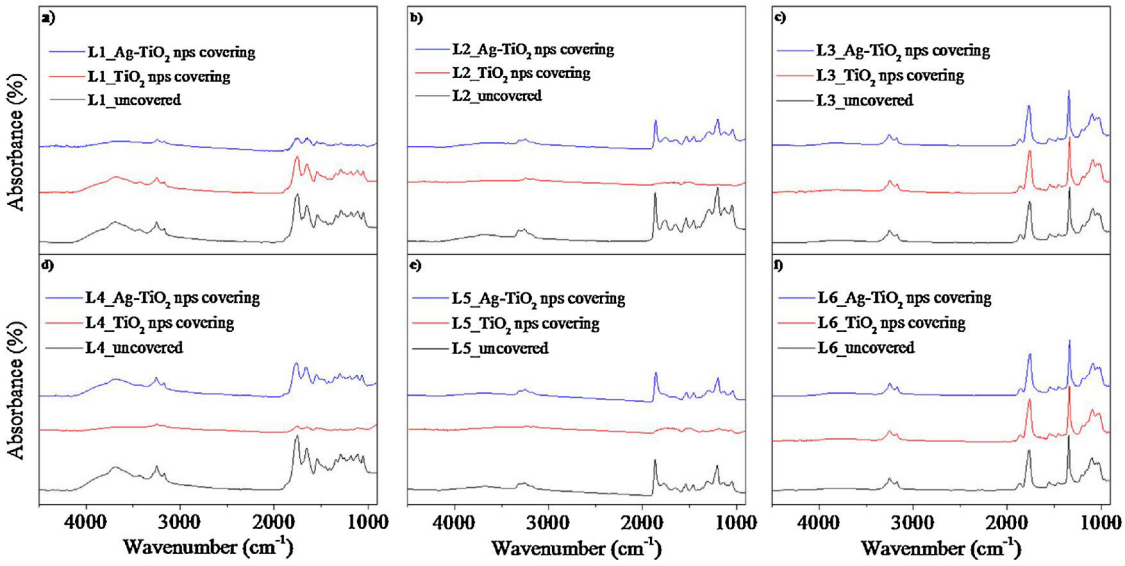

Fig. 6. FTIR spectra of six leathers pieces (L1, L2, L3, L4, L5 and L6) uncovered and covered with TiO_2 and Ag–TiO_2 nanoparticles.

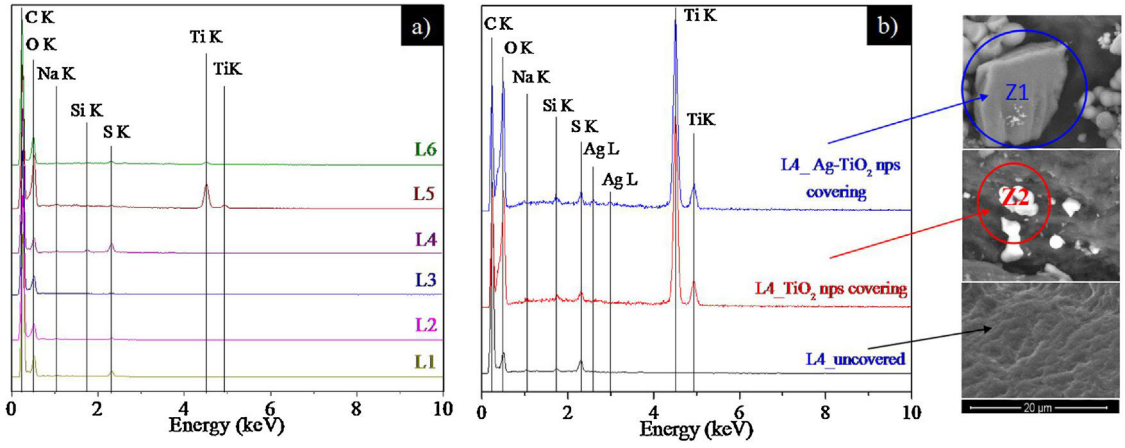

Fig. 7. EDX analyses of: (a) six leathers pieces uncovered (L1–L6) and (b) piece 4 (L4) uncovered and covered with TiO_2 and Ag–TiO_2 nanoparticles. SEM micrograph of EDX analysis on aggregate zone.

sample covered with Ag–TiO_2 NPs shows a weak peak of silver due to the presence of Ag on the surface of the NPs. The regions where the EDX spectra were acquired are depicted in the SEM images enclosed on the right part of Fig. 7b, where the presence of the brighter NPs on top of the darker leather can be observed.

Additional information about the presence and distribution of NPs on the surface of L4 can be obtained in Fig. 8. Fig. 8a and b show the pristine surface of L4 sample prior to NPs coverage at two different magnifications. In contrast, the appearance of bright agglomerates (of several microns in size) can be detected in Fig. 8c and e, as observed in the images acquired at high magnification (Fig. 8d and f), which is much larger than the values obtained by XRD and TEM. It is clear that there is room for improving the uniformity of the NPs distribution on the surface of the leathers, by optimization of the dispersion of the NPs in the solution and the incorporation process on a substrate of complex topography. Nonetheless, it is worth mentioning that small bright spots can also be identified in these latter images, which were not observed in the images of the pristine samples (Fig. 8a), which are probably non-agglomerated NPs.

3.2.2. *Antimicrobial properties*

Fig. 9 shows the halo tests carried out in pieces L1–L6 using *P. aeruginosa* (top), *S. aureus* (center), and *C. albicans* (bottom), respectively. Test performed to uncovered samples (left), samples covered with TiO_2 nanoparticles (center) and covered with Ag–TiO_2 nanoparticles (right) are depicted. The antibacterial activity ascribed to Ag can be clearly appreciated in the well-defined halos around all leathers (14 ± 1.0 mm) in Fig. 9c, while no inhibition zone is observed in Fig. 9a and b.

It is worth mentioning that uncovered leathers L1 and L4 (Fig. 9d) exhibited a little zone of inhibition (11 ± 0.2 mm),

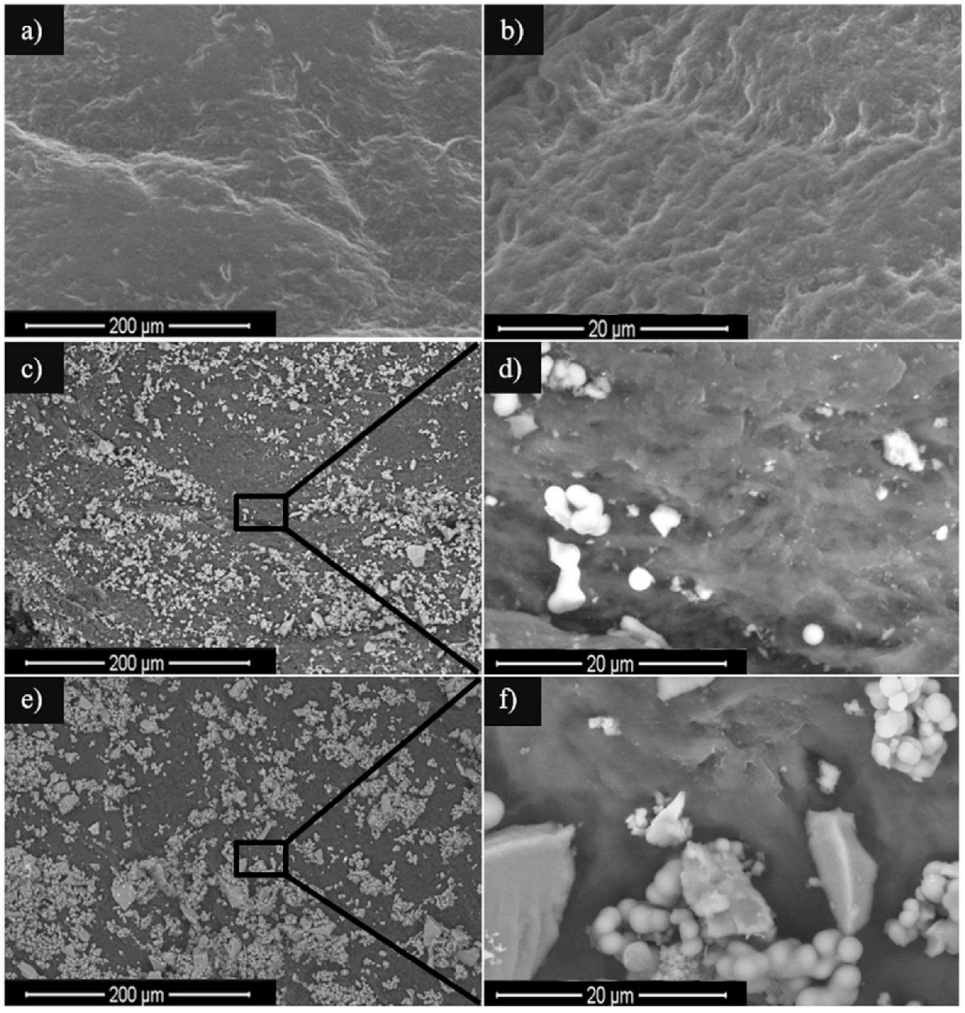

Fig. 8. SEM micrographs of piece L4: (a) and (b) uncovered, (c) and (d) covered with TiO_2 nanoparticles (BSE images), and (e) and (f) covered with Ag–TiO_2 nanoparticles (BSE images).

indicating an antibacterial activity against *S. aureus*, contrary to what observed against *P. aeruginosa*. This interesting result can be explained when considering the cell wall of the bacteria; the *S. aureus* (Gram positive) has a thicker layer of peptidoglycans, but it is simpler than the Gram negative wall of the *P. aeruginosa*, which has an additional outer membrane with lipopolysaccharides and may prevent the entry of the chemicals present in the initial treatment of leathers (cf. Table 1). In the other samples, no antibacterial activity was observed, possibly due to the presence of the base coat and the applied fixing layer (cf. Table 1).

All samples covered with TiO_2 NPs do not exhibit halo against *S. aureus* (Fig. 9e), probably because the nanoparticles covered the surface of the samples and avoid the influence of the chemicals in the growth of the bacteria. Finally, all samples covered with Ag–TiO_2 (Fig. 9f) showed halos of inhibition (12 ± 0.8 mm), indicating again the antibacterial activity of Ag. The antifungal properties are studied in the bottom part of Fig. 9. It was observed that all the uncovered samples showed antifungal activity (Fig. 9g). Nevertheless, samples L1 and L4 showed the greatest zones of inhibition (17 ± 0.7 mm), followed by the L2 and L5 (15 ± 0.8 mm), and L3 and L6 (13 ± 0.7 mm). This is likely explained by the chemicals present in the initial treatment of the leathers, which are mostly antifungal. The acrylic polymer base coating and nitrocellulose fixative present in samples L3 and L6 may serve as a partial barrier to the diffusion of antifungal agents, which explains the comparably lower antifungal activity. The lack of fixative, the diffusion of the antifungal agents will be more facilitated and L4 have the largest zone of inhibition due to the absence of any type of base coatings.

Samples covered with TiO_2 NPs (Fig. 9h) do not show halo of inhibition around them. As happened in the case of the *S. aureus* (Fig. 9e), possibly the TiO_2 NPs can cover and avoid the diffusion of chemicals from the surface of the leathers. Finally, Fig. 9i shows large diffuse halos (17 ± 0.9 mm) around all the Ag–TiO_2 covered samples. In agreement with what observed with the bacteria, since the samples with TiO_2 NPs showed no antifungal activity, these diffuse halos are a consequence of the antimicrobial properties of silver.

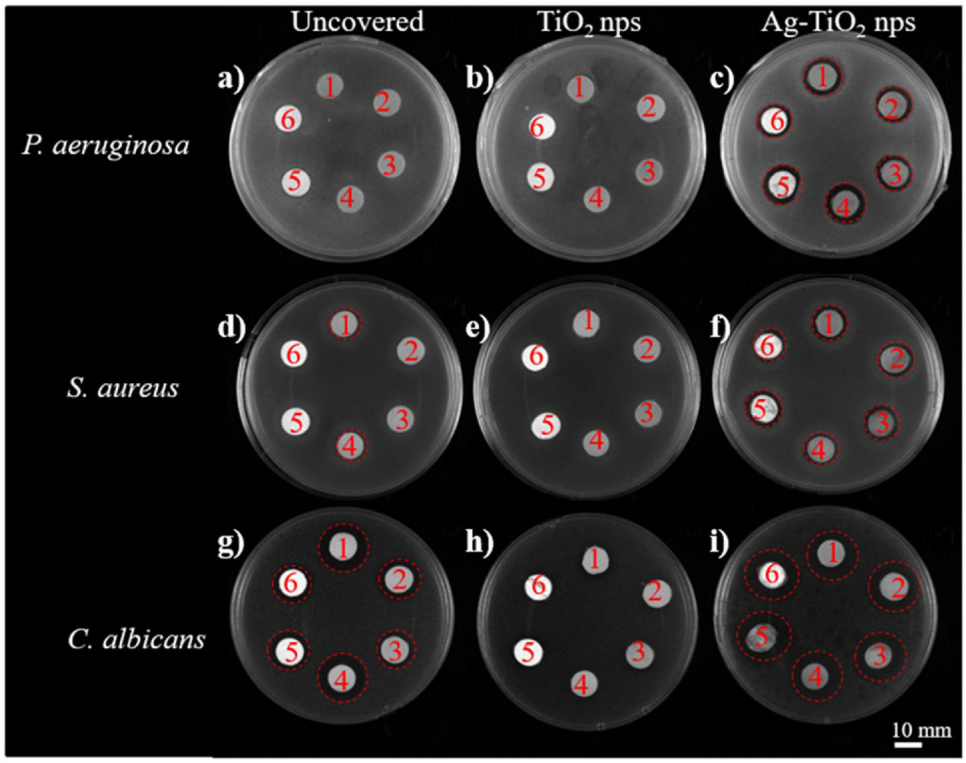

Fig. 9. Halo test of Leathers 1–6 using *P. aeruginosa*, *S. aureus* and *C. albicans* (top, center and bottom, respectively). The red circles highlight samples with the halo inhibition.

4. Conclusion

An innovative, simple and reliable method of synthesis has been used to prepare TiO_2 and Ag–TiO_2 nanoparticles with anatase phase. Those nanoparticles were dispersed in leather substrates with different surface finishing. It was demonstrated that nanoparticles stayed on the surface after water washing, although large agglomerates are observed. All leather samples covered with Ag–TiO_2 nanoparticles showed antimicrobial activity, in contrast with samples covered with TiO_2 nanoparticles. Therefore, silver is identified as the main antimicrobial agent. Moreover, a low toxicity of Ag–TiO_2 nanoparticles was demonstrated by cytotoxicity assays, displaying a death cell percentage inferior to 30%. Therefore, this work highlighted the potential of Ag–TiO_2 nanoparticles as an ecological alternative to volatile organic biocides and organic solvents, frequently used nowadays, and it was an essential step toward the assessment of a safe application of these NMs. This study brings added value to footwear and leather products, reducing the bulk chemical wide pollution.

Acknowledgments

This research is sponsored by FEDER funds through the program COMPETE – Programa Operacional Factores de Competitividade and by the Portuguese Foundation for Science and Technology (FCT) in the framework of the Strategic Funding UID/FIS/04650/2013, and UID/EMS/00285/2013 and in the framework of ERA-SIINN/0004/2013 project.

References

[1] K. Kolomaznik, M. Adamek, I. Andel, M. Uhlirova, Leather waste – potential threat to human health, and a new technology of its treatment, J. Hazard. Mater. 160 (2008) 514–520, http://dx.doi.org/10.1016/J.JHAZMAT.2008.03.070.

[2] C. Lok, C. Ho, R. Chen, Q. He, W. Yu, H. Sun, P.K. Tam, J. Chiu, C. Che, Proteomic analysis of the mode of antibacterial action of silver nanoparticles research articles, J. Proteome Res. 5 (2006) 916–924.

[3] J.S. Kim, E. Kuk, K.N. Yu, J.H. Kim, S.J. Park, H.J. Lee, S.H. Kim, Y.K. Park, Y.H. Park, C.Y. Hwang, Y.K. Kim, Y.S. Lee, D.H. Jeong, M.H. Cho, Antimicrobial effects of silver nanoparticles, Nanomed. Nanotechnol. Biol. Med. 3 (2007) 95–101, http://dx.doi.org/10.1016/j.nano.2006.12.001.

[4] S. Jaiswal, P. McHale, B. Duffy, Preparation and rapid analysis of antibacterial silver, copper and zinc doped sol-gel surfaces, Colloids Surf. B: Biointerfaces 94 (2012) 170–176, http://dx.doi.org/10.1016/j.colsurfb.2012.01.035.

[5] U. Samuel, J.P. Guggenbichler, Prevention of catheter-related infections: the potential of a new nano-silver impregnated catheter, Int. J. Antimicrob. Agents 23 (2004) 75–78, http://dx.doi.org/10.1016/j.ijantimicag.2003.12.004.

[6] K. Chaloupka, Y. Malam, A.M. Seifalian, Nanosilver as a new generation of nanoproduct in biomedical applications, Trends Biotechnol. 28 (2010) 580–588, http://dx.doi.org/10.1016/j.tibtech.2010.07.006.

[7] Y. Hsin, C. Chen, S. Huang, T. Shih, P. Lai, P. Ju, The apoptotic effect of nanosilver is mediated by a ROS- and JNK-dependent mechanism involving the mitochondrial pathway in NIH3T3 cells, Toxicol. Lett. 179 (2008) 130–139, http://dx.doi.org/10.1016/j.toxlet.2008.04.015.

[8] S. Park, Y.K. Lee, M. Jung, K.H. Kim, N. Chung, E.-K. Ahn, Y. Lim, K.-H. Lee, Cellular toxicity of various inhalable metal nanoparticles on human alveolar epithelial cells, Inhal. Toxicol. 19 (Suppl. 1) (2007) 59–65, http://dx.doi.org/10.1080/08958370701493282.

[9] A. Petica, C. Gaidau, J. Ma, D. Simion, Q. Xu, M. Niculescu, Antimicrobial electrochemically obtained nanosilver solutions for leather and furskin treatment, Rev. Chim. 64 (2013) 1329–1334.

[10] I.M. Lopez, M.F. Payà-Nohales, J.N. Cuesta-Garrote, F. Arán-Ais, M.Á. Martinez-Sánchez, C. Orgilés-Barceló, M. Bertazzo, Antimicrobial effect of coated leather based on silver nanoparticles and nanocomposites: synthesis, characterisation and microbiological evaluation, J. Biotechnol. Biomater. 05 (2015) 1–10, http://dx.doi.org/10.4172/2155-952X.1000171.

[11] M.M. Sanchez-Navarro, M.A. Perez-Liminana, N. Cuesta-Garrote, M.I. Maestre-Lopez, M. Bertazzo, M.A. Martinez-Sanchez, C. Orgiles-Barcelo, F. Aran-Ais, Latest developments in antimicrobial functional materials for footwear, in: Microbial Pathogens and Strategies for Combating Them: Science, Technology and Education, 2013, pp. 102–113.

[12] P. Velmurugan, S.M. Lee, M. Cho, J.H. Park, S.K. Seo, H. Myung, K.S. Bang, B.T. Oh, Antibacterial activity of silver nanoparticle-coated fabric and leather against odor and skin infection causing bacteria, Appl. Microbiol. Biotechnol. 98 (2014) 8179–8189, http://dx.doi.org/10.1007/s00253-014-5945-7.

[13] A. Fujishima, X. Zhang, D.A. Tryk, TiO_2 photocatalysis and related surface phenomena, Surf. Sci. Rep. 63 (2008) 515–582, http://dx.doi.org/10.1016/j.surfrep.2008.10.001.

[14] S.M. Gupta, M. Tripathi, A review of TiO_2 nanoparticles, Chin. Sci. Bull. 56 (2011) 1639–1657, http://dx.doi.org/10.1007/s11434-011-4476-1.

[15] V.I. Shapovalov, Nanopowders and films of titanium oxide for photocatalysis: a review, Glas. Phys. Chem. 36 (2010) 121–157, http://dx.doi.org/10.1134/S108765961002001X.

[16] J.W. Liou, H.H. Chang, Bactericidal effects and mechanisms of visible light-responsive titanium dioxide photocatalysts on pathogenic bacteria, Arch. Immunol. Ther. Exp. (Warsz) 60 (2012) 267–275, http://dx.doi.org/10.1007/s00005-012-0178-x.

[17] S. Sönmezoglu, Processing and electrical characterization of metal-oxide-semiconductor structures prepared by DBSA – doped TiO_2 nanoparticles, Curr. Nanosci. 9 (2013) 39–45.

[18] M.Z. Yahaya, M.Z. Abdullah, A.A. Mohamad, Centrifuge and storage precipitation of TiO_2 nanoparticles by the sol-gel method, J. Alloys Compd. 651 (2015) 557–564, http://dx.doi.org/10.1016/j.jallcom.2015.08.110.

[19] W. Kongsuebchart, P. Praserthdam, J. Panpranot, A. Sirisuk, P. Supphasrirongjaroen, C. Satayaprasert, Effect of crystallite size on the surface defect of nano-TiO_2 prepared via solvothermal synthesis, J. Cryst. Growth 297 (2006) 234–238, http://dx.doi.org/10.1016/j.jcrysgro.2006.09.018.

[20] Y. Yuan, J. Ding, J. Xu, J. Deng, J. Guo, TiO_2 nanoparticles co-doped with silver and nitrogen for antibacterial application, J. Nanosci. Nanotechnol. 10 (2010) 4868–4874, http://dx.doi.org/10.1166/jnn.2010.2225.

[21] S. Khan, I.A. Qazi, I. Hashmi, M.A. Awan, N.U.S.S. Zaidi, Synthesis of silver-doped titanium TiO_2 powder-coated surfaces and its ability to inactivate *Pseudomonas aeruginosa* and *Bacillus subtilis*, J. Nanomater. 2013 (2013), http://dx.doi.org/10.1155/2013/531010.

[22] X.H. Yang, H.T. Fu, X.C. Wang, J.L. Yang, X.C. Jiang, A.B. Yu, Synthesis of silver-titanium dioxide nanocomposites for antimicrobial applications, J. Nanopart. Res. 16 (2014), http://dx.doi.org/10.1007/s11051-014-2526-8.

[23] A.W. Bauer, W.M. Kirby, J.C. Sherris, M. Turck, Antibiotic susceptibility testing by a standardized single disk method, Am. J. Clin. Pathol. 45 (1966) 493–496.

[24] M. Rehan, X. Lai, G.M. Kale, Hydrothermal synthesis of titanium dioxide nanoparticles studied employing in situ energy dispersive X-ray diffraction, CrystEngComm 13 (2011) 3725, http://dx.doi.org/10.1039/c0ce00781a.

[25] International Organization for Standardization, Biological Evaluation of Medical Devices – Part 5: Tests for In Vitro Cytotoxicity. ISO 10993-5, vol. 5, 2009, pp. 1–52.

[26] L. Falcão, M.E.M. Araújo, Application of ATR–FTIR spectroscopy to the analysis of tannins in historic leathers: the case study of the upholstery from the 19th century Portuguese Royal Train, Vib. Spectrosc. 74 (2014) 98–103, http://dx.doi.org/10.1016/j.vibspec.2014.08.001.

[27] G. Duan, C. Zhang, A. Li, X. Yang, L. Lu, X. Wang, Preparation and characterization of mesoporous zirconia made by using a poly (methyl methacrylate) template, Nanoscale Res. Lett. 3 (2008) 118–122, http://dx.doi.org/10.1007/s11671-008-9123-7.

[28] V.I. Kovalenko, R.M. Mukhamadeeva, L.N. Maklakova, N.G. Gustova, Interpretation of the IR spectrum and structure of cellulose nitrate, J. Struct. Chem. 34 (1994) 540–547, http://dx.doi.org/10.1007/BF00753522.